ELSEVIER

Alcohol 35 (2005) 3–12

ALCOHOL

Theoretical article

A physiologically based model for ethanol and acetaldehyde metabolism in human beings

David M. Umulis[1], Nihat M. Gürmen, Prashant Singh, H. Scott Fogler*

University of Michigan, Department of Chemical Engineering, 2300 Hayward Street, Ann Arbor, MI 48109-2136, USA

Received 19 August 2004; received in revised form 2 November 2004; accepted 7 November 2004

Abstract

Pharmacokinetic models for ethanol metabolism have contributed to the understanding of ethanol clearance in human beings. However, these models fail to account for ethanol's toxic metabolite, acetaldehyde. Acetaldehyde accumulation leads to signs and symptoms, such as cardiac arrhythmias, nausea, anxiety, and facial flushing. Nevertheless, it is difficult to determine the levels of acetaldehyde in the blood or other tissues because of artifactual formation and other technical issues. Therefore, we have constructed a promising physiologically based pharmacokinetic (PBPK) model, which is an excellent match for existing ethanol and acetaldehyde concentration–time data. The model consists of five compartments that exchange material: stomach, gastrointestinal tract, liver, central fluid, and muscle. All compartments except the liver are modeled as stirred reactors. The liver is modeled as a tubular flow reactor. We derived average enzymatic rate laws for alcohol dehydrogenase (ADH) and acetaldehyde dehydrogenase (ALDH), determined kinetic parameters from the literature, and found best-fit parameters by minimizing the squared error between our profiles and the experimental data. The model's transient output correlates strongly with the experimentally observed results for healthy individuals and for those with reduced ALDH activity caused by a genetic deficiency of the primary acetaldehyde-metabolizing enzyme *ALDH2*. Furthermore, the model shows that the reverse reaction of acetaldehyde back into ethanol is essential and keeps acetaldehyde levels approximately 10-fold lower than if the reaction were irreversible.

Keywords: Alcohol metabolism; Acetaldehyde dehydrogenase (ALDH); ALDH deficiency; Physiologically based pharmacokinetic (PBPK) model; Alcohol dehydrogenase (ADH); Michaelis–Menten kinetics

1. Introduction

Pharmacokinetic models for in vivo ethanol elimination have evolved significantly during the past 70 years, from the inception of a pseudo zero-order elimination process (Widmark, 1932) to the current physiologically based models such as those developed by Derr (1993), Levitt (2002), and Norberg (2001). Although the models continually improve in their ability to predict time trajectories for ethanol concentration, they fail to account for the production and interaction of ethanol's major metabolite, acetaldehyde. Acetaldehyde is highly toxic, with a 50% lethal dose (LD_{50}) concentration approximately 10 times lower than that for ethanol in rats (Brien & Loomis, 1983). Acetaldehyde exposure leads to a number of well-known signs and symptoms, such as cardiac arrhythmias, nausea, anxiety, and facial flushing (Condouris & Havelin, 1987; Peng et al., 1999; Yamamoto et al., 2000).

In this article, we present a physiologically based model with reversible enzyme kinetics that accurately predicts simultaneously the concentrations of both ethanol and acetaldehyde in the blood as a function of time.

2. Methods

2.1. Rate law derivation

The rate law for ethanol metabolism is based on the alcohol dehydrogenase (ADH) reaction pathway because it is the largest contributor to ethanol oxidation.

The first assumption is that the concentration of the oxidized form of nicotinamide adenine dinucleotide (NAD^+) reaches its rate-limiting state shortly after ingestion and remains constant. Ethanol elimination is approximately zeroth order, supporting the suggestion that the reaction is limited by the amount of enzyme, co-substrate, or both. The enzymatic reaction, accounting for the NAD^+ co-substrate, is

* Corresponding author. Tel.: +1-734-763-1361; fax: +1-734-763-0459.
E-mail address: sfogler@umich.edu (H.S. Fogler).
[1] Present address: University of Minnesota, Department of Chemical Engineering and Materials Science, 421 Washington Avenue SE, Minneapolis, MN 55455, USA.

Accepting Editor: T.R. Jerrells

0741-8329/05/$ – see front matter © 2005 Elsevier Inc. All rights reserved.
doi: 10.1016/j.alcohol.2004.11.004

$$r_{Al} = \frac{V_m{}^*(S_1)(S_2)}{K_{12} + K_1(S_1) + K_2(S_2) + (S_1)(S_2)}$$

where $S_1 \equiv C_{Alcohol}$, and $S_2 \equiv C_{NAD^+}$.

Thus, because the elimination is approximately constant with rate V_{max}, two cases are possible: The rate occurs at $V_{max} = V_m$ when S_1 is $\gg K_2$ and NAD^+ is either in excess such that $(K_{12}+K_1S_1)/S_2$ approaches zero or the rate occurs at $V_{max} = f(S_2)$ and S_2 reaches a limiting concentration dependent on the rate that it is replenished to the system. In this situation, the experimentally observed K_M and V_{max} depend on the steady-state concentration of NAD^+:

$$r_{Al} = \frac{\frac{V_m(S_2)}{K_1 + (S_2)} * (S_1)}{\frac{K_{12} + K_2(S_2)}{K_1 + (S_2)} + (S_1)}$$

where $K_M \equiv \frac{K_{12} + K_2(S_2)}{K_1 + (S_2)}$, and $V_{max*} \equiv \frac{V_{max}(S_2)}{K_1 + (S_2)}$

It is most likely that the concentration of NAD^+ is limiting, but the exact levels are not necessary for this study. Instead, it is worth noting that V_{max} and K_m depend on the steady-state concentrations of NAD^+.

The second assumption is that the net rate of formation of the substrate–enzyme complex is zero. Consequently, we can apply the pseudo steady state hypothesis (PSSH) to the enzyme–ethanol and enzyme–acetaldehyde complexes (Fogler, 1999).

The derivation of the rate law for acetaldehyde oxidation is similar to the derivation for ethanol oxidation with one major exception: Acetaldehyde oxidation to acetate is not reversible. The rate law is based on the mitochondrial class 2 aldehyde dehydrogenase (*ALDH2*) enzymatic pathway because it is the largest contributor to acetaldehyde oxidation. In healthy human beings, *ALDH2* activity alone accounts for more than 99% of acetaldehyde oxidation (Riveros-Rosas et al., 1997). *ALDH2* uses the same co-substrate, NAD^+, as ADH, and therefore it is assumed to reach its rate-limiting state rapidly and to remain constant at that level. The derivation of the acetaldehyde oxidation rate law is also based on application of the PSSH to the enzyme–substrate complexes.

Balance equations and rate law derivation are shown in Fig. 1A (Fogler, 1999). C_{Al} is the ethanol concentration, and C_{Ac} is the acetaldehyde concentration. V_{maxADH} is the maximum enzymatic oxidation rate of ethanol, V_{revADH} is the maximum rate of the reverse reaction of acetaldehyde to ethanol, and K_{mADH} and K_{revADH} are reaction constants for the rate law. The rate law for acetaldehyde oxidation depends only on the concentration of acetaldehyde and follows classical Michaelis–Menten kinetics.

2.2. Physiologically based model

We consider our system to be lumped into five organ compartments that exchange material. The five compartments are the stomach, gastrointestinal tract, liver, central fluid, and muscle. The stomach compartment in this model contains zero tissue water volume and only the volume of the liquid contents (alcoholic beverage), which is absorbed into the gastrointestinal compartment. The gastrointestinal compartment accounts for the tissue water volume of the intestines and the stomach where ethanol is first absorbed. We chose to separate the gastrointestinal compartment from the central compartment on the basis of physiologic connectivity. This separation also establishes a base case model that can be extended easily to studies on the role of the gastrointestinal tract in first-pass metabolism. A perfusion-limited model was selected because both ethanol and acetaldehyde are small molecules with rapid diffusion, and their distribution is limited by the rate they are transported to the tissues, not by the rate at which they are absorbed.

Physiologically based models have available to them the human approximations for tissue water volume, perfusion rates, and tissue water distribution (well-mixed vs. concentration gradient). Such data are given in Table 1 for a "standard" 69.4-kg man whose total body water content is 40.8 l (Rowland et al., 1995).

To accurately describe ethanol and acetaldehyde metabolism in vivo, we divided the total tissue water volume of an average 69.4-kg male human being into three well-mixed compartments and one tubular flow compartment. Organ volumes were lumped into compartments on the basis of three criteria: (1) perfusion rate of fluid through each organ, (2) physical connectivity between organs, and (3) ethanol and acetaldehyde metabolic activity. The perfusion rate is defined as the flow rate to and from the organ per unit volume of tissue, and the inverse of the perfusion rate is the residence time. Ethanol and acetaldehyde metabolism occurs within the liver, which was considered as a tubular flow reactor on the basis of early kinetic results obtained by Keiding and Priisholm (1984). The stomach and intestine water volumes were grouped into the gastrointestinal compartment because they are connected directly to the liver by means of the hepatic portal vein and because they are the sites of ethanol absorption from an external source. Finally, organs with a perfusion rate of greater than 0.08 ml/min/ml H_2O were placed within the central compartment, whereas organs with perfusion rates of less than 0.08 ml/min/ml H_2O were placed within the muscle compartment.

Mass balance equations with the appropriate reaction rate laws were constructed on the basis of flow of blood between compartments and are shown in Fig. 1B. The compartment labeled "Stomach" contains the ethanol that is external to the body and represents the volume of the liquid contents (alcoholic beverage) that is absorbed into the gastrointestinal compartment. Fig. 2A shows the compartment/flow diagram for the model. The rate of stomach emptying, determined by using radiopharmaceuticals by Levitt and Levitt (1994), can be approximated by a first-order linear ordinary differential equation, where the rate of removal

A.

ethanol

$$CH_3CH_2OH + ADH \leftrightarrow CH_3CH_2OH \bullet ADH$$
NAD+/NADH

$$CH_3CH_2OH \bullet ADH \leftrightarrow CH_3CHO \bullet ADH + H_2O$$
NAD+/NADH

$$CH_3CHO \bullet ADH \leftrightarrow CH_3CHO + ADH$$

$$-r_{Al} = \frac{Vmax_{ADH}(C_{Al}) - Vrev_{ADH}(C_{Ac})}{Km_{ADH} + (C_{Al}) + Krev_{ADH}(C_{Ac})}$$

$-r_{Al}$ = rate of dissapearance of ethanol

acetaldehyde

$$CH_3CHO + ALDH \leftrightarrow CH_3CHO \bullet ALDH$$
NAD+/NADH

$$H_2O + CH_3CHO \bullet ALDH \leftrightarrow CH_3COOH \bullet ALDH$$
NAD+/NADH

$$CH_3CHOOH \bullet ALDH \rightarrow CH_3COOH + ALDH$$

$$-r_{Ac} = \frac{Vmax_{ALDH}(C_{Ac})}{Km_{ALDH} + (C_{Ac})}$$

$-r_{Ac}$ = rate of dissapearance of acetaldehyde

B.

Stomach Compartment

$$\left(\frac{dV_S}{dt}\right) = -k_S(V_S)$$

k_S = stomach-emptying rate constant
V_S = volume of fluid in the stomach

ethanol

$$V_G \frac{dC_{GAl}}{dt} = \left(\frac{2}{3}v_L\right)(C_{CAl} - C_{GAl}) + k_S(V_S)(C_{SAl})$$

acetaldehyde

$$V_G \frac{dC_{GAc}}{dt} = \left(\frac{2}{3}v_L\right)(C_{CAc} - C_{GAc})$$

Gastrointestinal Compartment

Liver Compartment

$$\Delta V_L \frac{dC_{NAl}}{dt} = v_L(C_{(N-1)Al} - C_{NAl}) + r_{Al}(C_{NAl}, C_{NAc})\Delta V_L$$

$$\Delta V_L \frac{dC_{NAc}}{dt} = v_L(C_{(N-1)Ac} - C_{NAc}) - r_{Al}(C_{NAl}, C_{NAc})\Delta V_L + r_{Ac}(C_{NAc})\Delta V_L$$

Central Compartment

$$V_C\left(\frac{dC_{CAl}}{dt}\right) = -v_L(C_{CAl} - C_{LAl}) - v_M(C_{CAl} - C_{MAl})$$

$$V_C\left(\frac{dC_{CAc}}{dt}\right) = -v_L(C_{CAc} - C_{LAc}) - v_M(C_{CAc} - C_{MAc})$$

Muscle Compartment

$$V_M\left(\frac{dC_{MAl}}{dt}\right) = v_M(C_{CAl} - C_{MAl})$$

$$V_M\left(\frac{dC_{MAc}}{dt}\right) = v_M(C_{CAc} - C_{MAc})$$

v_L = liver flow rate
V_i = tissue water volume in i-th compartment

C_{iAl} = ethanol concentration in i-th compartment
C_{iAc} = acetaldehyde concentration in i-th compartment

Fig. 1. A. Derivation of rate laws for ethanol and acetaldehyde. B. Mass balance equations for physiologically based model. A, left panel: adapted from F. Lundquist and H. Wolthers, The kinetics of alcohol elimination in man, *Acta Pharmacologica Et Toxicologica 14(3)*, pp. 265–289, copyright 1958, with permission of Blackwell Publishing. A, right panel: adapted from *Archives of Medical Research 28(4)*, H. Riveros-Rosas, A. Julian-Sanchez, and E. Pina, Enzymology of ethanol and acetaldehyde metabolism in mammals, pp. 453–471, copyright 1997, with permission from ***IMSS***. ADH = Alcohol dehydrogenase; ALDH = acetaldehyde dehydrogenase, NAD^+ = oxidized form of nicotinamide adenine dinucleotide; NADH = reduced form of nicotinamide adenine dinucleotide.

is proportional to the volume of stomach contents (Levitt & Levitt, 1994). However, the stomach-emptying rate constant depends on the osmotic pressure of the stomach contents, and ethanol increases the osmotic pressure. Wilkinson et al. (1977) have shown that the rate constant is a nonlinear function of the initial dose of ethanol ingested. The equation previously proposed and used for this work is $k_S = k_{Smax}/(1+a(D)^2)$, where k_S is the stomach-emptying rate constant, k_{Smax} is the maximum stomach-emptying rate constant, a is an empirical parameter, and D is the initial dose (mmol) of ethanol in the stomach.

It is quite difficult to determine the concentration of free acetaldehyde in the blood on the basis of either breath or blood analysis methods. Artifactual formation of acetaldehyde

Table 1
Tissue water volumes, blood flow rates, and perfusion rates for the "standard" 69.4-kg man

Compartment	Tissue	H_2O volume (l)	Blood flow (ml/min)	Perfusion rate (ml/min/ml H_2O)	Residence time (min)	Source
Central $V_C = 11.56$ l	Lungs	0.37	5,000	13.33	0.07	a
	Kidneys	0.21	1,100	5.14	0.19	a
	Blood	2.84	5,000	1.76	0.57	a
	Brain	1.03	700	0.68	1.47	a
	Heart, spleen	1.18	350	0.29	3.37	a
	Bone	2.44	250	0.10	10.00	a
	Skin	3.49	300	0.085	11.63	a
Muscle	Fat	3.76	200	0.053	18.80	a
$V_M = 25.76$ l	Muscle	22.0	750	0.034	29.33	a
Gastrointestinal tract $V_G = 2.4$ l	Stomach/intestine	2.40	900	0.375	2.67	a,b
Liver $V_L = 1.08$ l	Liver	1.08	1,350	1.25	0.80	a,c

Total body water content is 40.8 l.

[a]Adapted from M. Rowland, T. N. Tozer, and R. Rowland, *Clinical Pharmacokinetics: Concepts and Applications* (3rd ed.), tbl. 6, copyright 1995, with permission of Lippincott Williams & Wilkins, www.lww.com.

[b]Adapted from R. F. Derr, Simulation studies on ethanol metabolism in different human populations with a physiological pharmacokinetic model, *Journal of Pharmaceutical Sciences 82(7)*, pp. 677–682, copyright 1993, with permission of Wiley-Liss and The American Pharmacists Association.

[c]Reproduced, with permission, from O. A. Larsen, K. Winkler, and N. Tygstrup, 1963, *Clinical Science 25(3)*, pp. 357–360, tbl. 4, © the Biochemical Society and the Medical Research Society.

inhibits accurate blood analysis, and production of acetaldehyde by microorganisms in the throat inhibits acetaldehyde determination from breath assays (Jones, 1995). Much of the acetaldehyde present in the blood is bound to plasma proteins and hemoglobin. Only the unbound acetaldehyde crosses the alveolar–capillary membranes of the lungs, and great care must be taken to ensure one is actually measuring free acetaldehyde. Breath tests give an approximation of free acetaldehyde in the blood; however, random errors in the assay used detract from the ability to accurately calculate blood acetaldehyde concentrations from breath levels. Noting these problems, we used breath acetaldehyde data in our initial analysis. To verify and test the model further, we compared our theoretical results with data obtained more recently by blood analysis in Asian men, for which recent protocols were used to reduce artifactual formation of acetaldehyde (Peng et al., 1999).

3. Results and discussion

3.1. Parameter values

The commercial technical computing package Matlab was used for model development and parameter estimation. The differential balances on each compartment, along with the appropriate enzymatic rate laws, were solved numerically with Matlab's stiff ordinary differential equation solvers because of the large difference in the ethanol and acetaldehyde concentrations (Shampine & Reichelt, 1997). Two realizations were carried out: (1) The model parameter values for the balance equations and rate laws were taken directly from the average literature values and (2) the model parameters were fit to the experimental concentration–time trajectories available in the literature. All parameter estimations were carried out by using Matlab's built-in routines from its optimization toolbox. A least square criterion between average experimental values and model output was used. As one can observe in Fig. 2B, 2C, and 2D, there is little variation between these two realizations. The model parameters are shown in Table 2. Because of the lack of a firmly established value, the Michaelis–Menten parameter V_{maxAc} was taken to be 2.7 mmol/(min*kg liver), which is within the range of the suggested values (Deetz et al., 1984).

In addition to the parameters in Table 2, k_{Smax} and a were fit to the model. Values of 0.05 min^{-1} and 1.22 mol^{-2} were obtained for k_{Smax} and a, respectively. Using these values for k_{Smax} and a, we obtained the overall stomach-emptying rate constants, in comparison with those from Wilkinson et al. (1977), shown in Table 3.

The absorption rate is much less dependent on the concentration of ethanol in the current model. In fact, for the 0.6-g/kg dose of ethanol, the results of our current studies indicate that 92% of the ethanol is absorbed within 100 min, whereas in the one-compartment model only 39% of the ethanol is absorbed. Even with very slow absorption rates, greater than 80% absorption is expected to occur within 100 min (Levitt & Levitt, 1994; Levitt et al., 1997).

3.2. Ethanol concentration

Fig. 2B shows a comparison of the ethanol concentration–time trajectories for the central compartment with the data obtained by Wilkinson et al. (1977). The four curves correspond to four different doses of ethanol being administered: 0.15, 0.3, 0.45, and 0.6 g/kg. One notes that in all

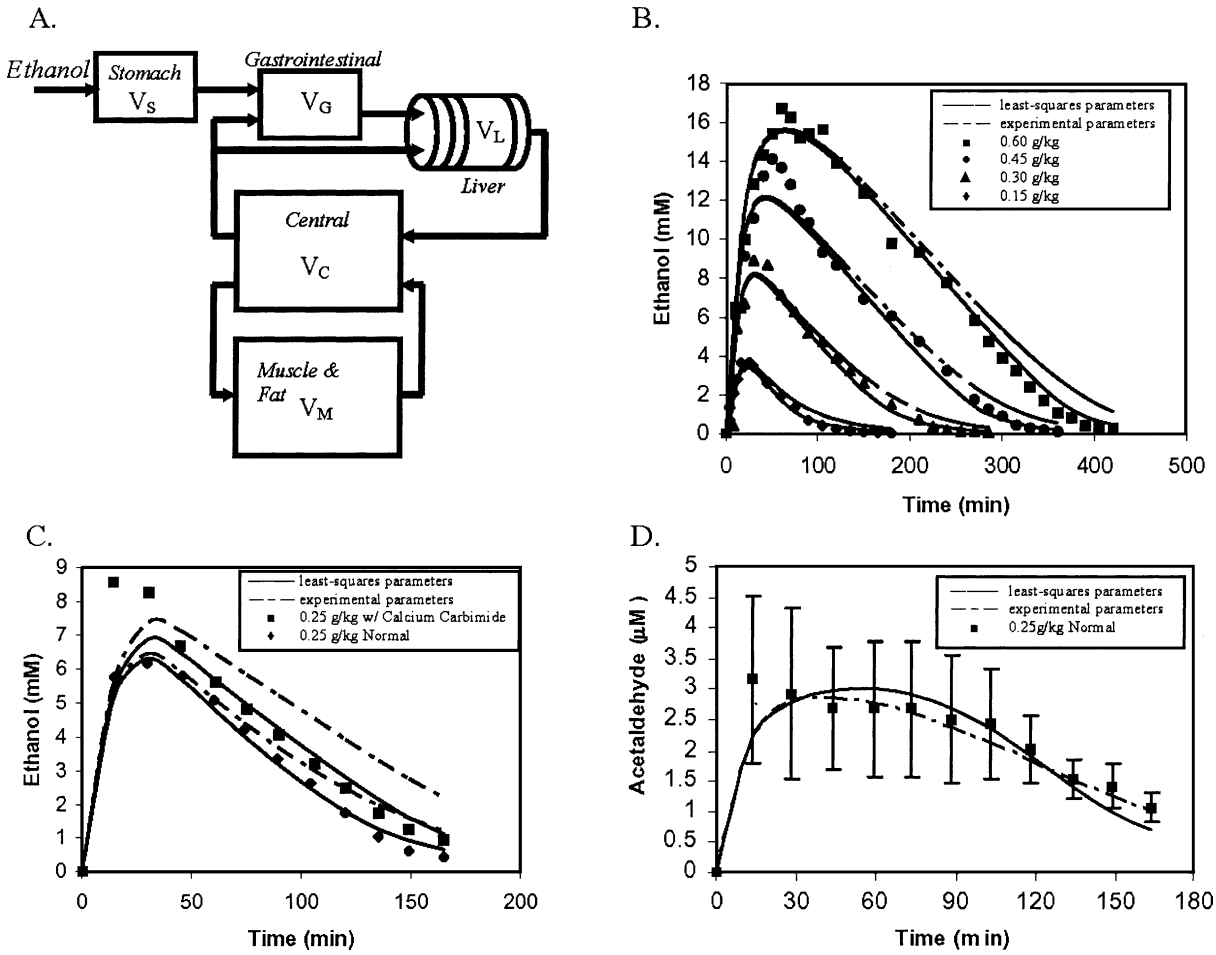

Fig. 2. A. Compartment and perfusion diagram for model. Perfusion interactions between compartments are shown by black arrows. V_G, V_L, V_C, and V_M are tissue water volumes for the gastrointestinal tract, liver, central compartment, and muscle and fat compartment, respectively. V_S is the stomach contents volume. B. Observed data (Wilkinson et al., 1977) versus model-predicted blood ethanol curves after ingestion of four different doses of ethanol in adult white male subjects. C. Observed data (Jones et al., 1988) versus model-predicted blood ethanol curves after ingestion of a 0.25-g/kg dose of 96% ethanol in 10 adult male subjects. D. Observed data (Jones et al., 1988) versus model-predicted blood acetaldehyde curve after ingestion of a 0.25-g/kg dose of ethanol in 10 adult male subjects. Error bars shown are one standard deviation of the mean of Jones et al. (1988) data. Note: All doses in panels B–D were adjusted from the 74.5-kg subjects to the "standard" 69.4-kg man used in the model. Observed data, panel B: adapted from P. K. Wilkinson, A. J. Sedman, E. Sakmar, D. R. Kay, and J. G. Wagner, Pharmacokinetics of ethanol after oral administration in the fasting state, *Journal of Pharmacokinetics and Biopharmaceutics 5(3)*, pp. 207–224, fig. 6, copyright 1977, with permission of Kluwer. Observed data, panels C and D: adapted from A. W. Jones, J. Neiman, and M. Hillbom, Concentration–time profiles of ethanol and acetaldehyde in human volunteers treated with the alcohol-sensitizing drug, calcium carbimide, *British Journal of Clinical Pharmacology 25(2)*, pp. 213–221, fig. 2 & fig. 3, copyright 1988, with permission of Blackwell Publishing.

cases there is excellent agreement between theory and experiment, as well as that the parameters taken from the literature give virtually the same result as those found by the least squares fit.

The correlation between the model predictions and experimental observations is excellent for ethanol, with an r^2 value of .98. One readily observes the model accurately predicts the ethanol concentration–time trajectory by using physiologically relevant parameters.

3.3. Alcohol dehydrogenase reverse reaction

The reverse reaction for acetaldehyde to ethanol in the blood is favored 5 to 50 times over acetaldehyde on the basis of in vitro calculations, supporting the notion of a significant reverse reaction effect (Deetz et al., 1984). To determine the influence of acetaldehyde on the removal of ethanol, we considered the data of Jones et al. (1988), who administered calcium carbimide in volunteers to slow the rate of acetaldehyde metabolism before giving them a dose of ethanol equivalent to 0.25 g of ethanol (96%) per kilogram of body weight. To calculate the value for the reverse reaction enzymatic activity parameter, V_{rev}, it was assumed that the concentration of acetaldehyde in the liver is equal to the concentration of acetaldehyde in the central compartment at time t. This approximation was made because of the lack of available data, and it introduces a minor amount of systematic error to our least squares fit estimate for V_{rev}. Fig. 2C shows a comparison of the suppressed metabolism and normal metabolism, along with the model prediction for each case. Theory and experiment are in good agreement, and

Table 2
Rate law parameters with the best model fit from least squares analysis in comparison with experimentally observed ranges and values used for the comparison plots

Parameter	Model	Experimental	Graph	Units	Source
V_{maxAl}	2.2	2.0, 2.4–4.7[†]	2.2	mmol*(min*kg liver)$^{-1}$	a,b
K_{mAl}	0.4	~1	1	mM	c
V_{rev}	32.6	11–110[‡]	60.5	mmol*(min*kg liver)$^{-1}$	d,e
K_{rev}	1	~1	1	mM/mM	d,e
V_{maxAc}	2.7	–	2.7	mmol*(min*kg liver)$^{-1}$	Estimate
K_{mAc}	1.2	0.2–3	1.6	μM	c,f

[†]Experimental values of 2.4 and 4.7 mmol*(min*kg liver)$^{-1}$ were observed at pH 8.5 and 10.5, respectively. Actual activity at physiologic liver pH of 7.5 is expected to be lower because pH 8.5 and 10.5 correspond to the optimal pH of two different forms of alcohol dehydrogenase.

[‡]Calculated on the basis of a 5- to 50-fold increase in kcat values of forward reaction $Vmax_{Al}$.

[a]Adapted from R. F. Derr, Simulation studies on ethanol metabolism in different human populations with a physiological pharmacokinetic model, *Journal of Pharmaceutical Sciences 82(7)*, pp. 677–682, copyright 1993, with permission of Wiley-Liss and The American Pharmacists Association.

[b]Adapted from H. A. W. Wynne, P. Wood, B. Herd, P. Wright, M. D. Rawlins, and O. F. W. James, The association of age with the activity of alcohol dehydrogenase in human liver, *Age and Ageing*, 1992, *21(6)*, pp. 417–420, tbl. Hepatic ADH activity, by permission of Oxford University Press.

[c]Adapted from *Archives of Medical Research 28(4)*, H. Riveros-Rosas, A. Julian-Sanchez, and E. Pina, Enzymology of ethanol and acetaldehyde metabolism in mammals, pp. 453–471, tbl. 4 & 6, copyright 1997, with permission from ***IMSS***.

[d]Adapted from *Alcohol 15(2)*, W. E. M. Lands, A review of alcohol clearance in humans, pp. 147–160, tbl.1, copyright 1998, with permission from ***IMSS***.

[e]Adapted with permission from J. S. Deetz, C. A. Luehr, and B. L. Vallee, Human liver alcohol dehydrogenase isozymes: reduction of aldehydes and ketones, *Biochemistry 23(26)*, pp. 6822–6828, tbl. II, copyright 1984 American Chemical Society.

[f]Adapted from G. S. Peng, M. F. Wang, C. Y. Chen, S. U. Luu, H. C. Chou, T. K. Li, and S. J. Yin, Involvement of acetaldehyde for full protection against alcoholism by homozygosity of the variant allele of mitochondrial aldehyde dehydrogenase gene in Asians, *Pharmacogenetics 9(4)*, pp. 463–476, copyright 1999, with permission of Lippincott Williams & Wilkins, http://lww.com.

the correlation between the model-predicted and experimentally observed results for the regular ethanol and calcium carbimide–inhibited *ALDH2* cases yields r^2 values of .99 and .89, respectively.

3.4. Acetaldehyde concentration

As discussed earlier, one of the salient features of the current model is that it can simultaneously predict the concentration–time trajectories for ethanol and acetaldehyde when they are measured simultaneously. Fig. 2C shows the ethanol comparison, and Fig. 2D shows the acetaldehyde comparison. There was no adjustment of parameter values for the different concentration trajectories. The results for blood acetaldehyde concentration–time trajectories predicted by the model are compared with experimental results obtained by Jones et al. (1988), after administration of a dose of ethanol equivalent to 0.25 g of ethanol (96%) per kilogram of body weight. Again, the agreement between the experiment measurements and the model is excellent. A correlation between the model-predicted and observed results for acetaldehyde is good, with an r^2 value of .88.

Table 3
Stomach-emptying rate constants

	Ethanol (g/kg)			
Study/source	0.15	0.3	0.45	0.6
Current work, k_S	0.047	0.040	0.032	0.025
Wilkinson et al.[a], k_S	0.055	0.018	0.009	0.005

[a]Adapted from P. K. Wilkinson, A. J. Sedman, E. Sakmar, D. R. Kay, and J. G. Wagner, Pharmacokinetics of ethanol after oral administration in the fasting state, *Journal of Pharmacokinetics and Biopharmaceutics 5(3)*, pp. 207–224, copyright 1977, with permission of Kluwer.

3.5. Acetaldehyde dehydrogenase deficiency

Another primary feature of the current model is its application to aldehyde dehydrogenase–deficient individuals to predict the acetaldehyde concentration–time trajectory. Acetaldehyde dehydrogenase activity in the liver was calculated by using data obtained from Enomoto et al. (1991), and it was based on the percent change from normal activity. Enomoto et al. (1991) showed that the total ALDH specific activity for acetaldehyde metabolism (V_{maxAc}) in heterozygous *ALDH2*1/*2* individuals was only 70% of the total ALDH specific activity for acetaldehyde metabolism (V_{maxAc}) in homozygous *ALDH2*1/*1* individuals for low doses of ethanol. In addition, the total ALDH specific activity for acetaldehyde metabolism (V_{maxAc}) in homozygous *ALDH2*2/*2* individuals was only 55% of the total ALDH specific activity for acetaldehyde metabolism (V_{maxAc}) in homozygous *ALDH2*1/*1* individuals. When we apply these percentages to our model V_{maxAc}, we get rates of 1.89 and 1.49 mmol*(min*kg liver)$^{-1}$ for *ALDH2*1/*2* and *ALDH2*2/*2* individuals, respectively. The results for heterozygous *ALDH2*1/*2* individuals are in agreement with the results shown by Wang et al. (1996). The Michaelis–Menten constant (K_m) was held constant, and only V_{maxAc} was varied.

These parameters were used in the model and compared with the data obtained from Peng et al. (1999) (Fig. 3A–3D), obtained by ethanol administration to *ALDH2*1/*1*, *ALDH2*1/*2*, and *ALDH2*2/*2* individuals (Peng et al., 1999; Wang et al., 1996). In addition, the stomach-emptying rate constant was reduced to 50% of the normal absorption rate because the subjects ate breakfast approximately 2 h before the study. In other studies (Jones et al., 1988; Wilkinson

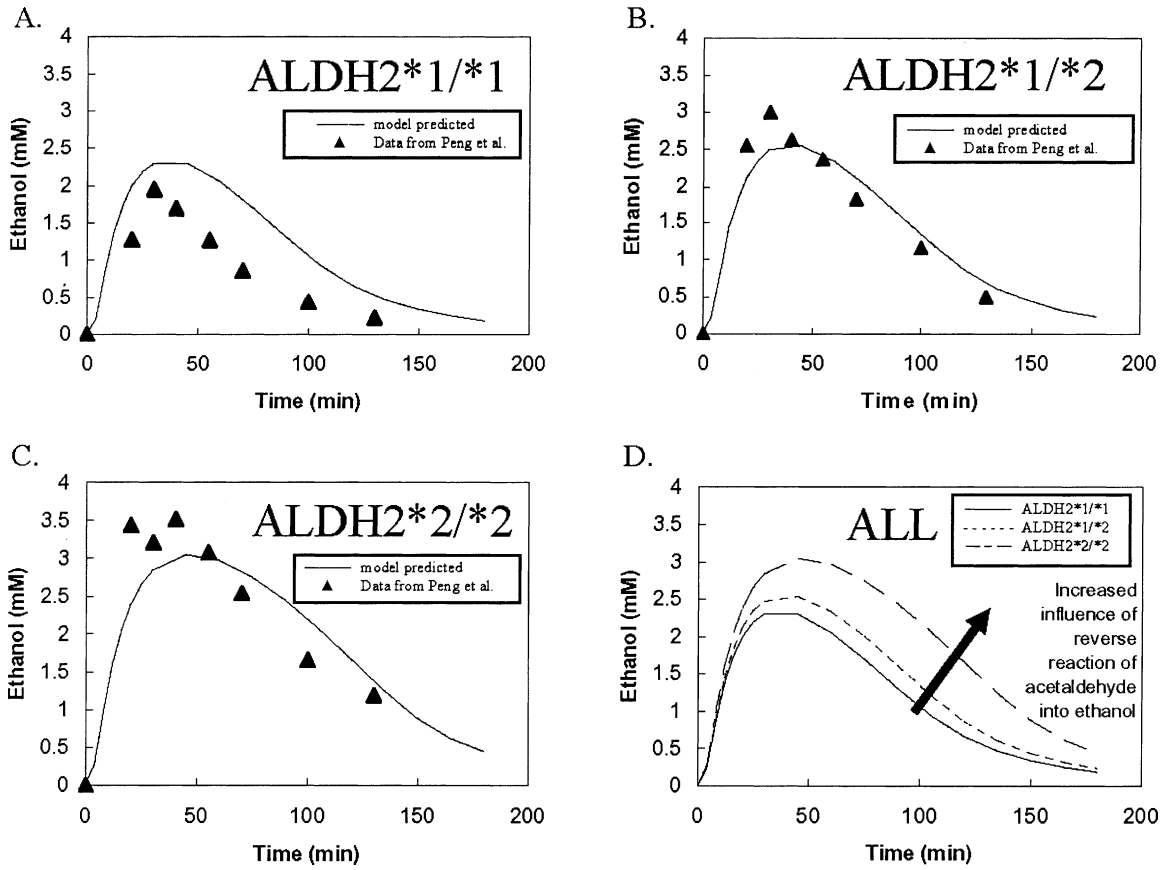

Fig. 3. Ethanol concentration results for model (———) versus data (▲) from Peng et al. (1999) after an equivalent 0.2-g/kg dose of ethanol in healthy (A) *ALDH2*1/*1*, (B) heterozygous *ALDH2*1/*2*, and (C) homozygous *ALDH2*2/*2* individuals. D. Comparison of the model-predicted ethanol concentration results from cases *ALDH2*1/*1* (———), *ALDH2*1/*2* (- - - - - -), and *ALDH2*2/*2* (— – —) to illustrate the effect of the reverse reaction of acetaldehyde to ethanol. Data (▲), panels A–C: adapted from G. S. Peng, M. F. Wang, C. Y. Chen, S. U. Luu, H. C. Chou, T. K. Li, and S. J. Yin, Involvement of acetaldehyde for full protection against alcoholism by homozygosity of the variant allele of mitochondrial aldehyde dehydrogenase gene in Asians, *Pharmacogenetics 9(4)*, pp. 463–476, fig. 1, copyright 1999, with permission of Lippincott Williams & Wilkins, http://lww.com.

et al., 1977), an overnight fast was required. This is calculated on the basis of the ethanol concentration–time data obtained by Lucey et al. (1999), after oral ingestion of ethanol at 0.3 g/kg in individuals after an overnight fast and consumption of a standard meal. The stomach-emptying rate constant decreases by approximately 50% after oral ingestion of ethanol at 0.3 g/kg after consumption of a standard meal. Plots of experimental data from Lucey et al. (1999), for fed and fasted states and model-predicted curves, are shown in Fig. 4D. Fig. 3 and Fig. 4A show the blood ethanol and blood acetaldehyde concentrations, respectively.

Fig. 4A shows acetaldehyde concentration–time trajectories for *ALDH2*1/*1* (bottom), *ALDH2*1/*2* (middle), and *ALDH2*2/*2* (top) individuals with data from Peng et al. (1999). As acetaldehyde concentration increases, the peak concentration becomes more distinct than is seen in lower acetaldehyde concentrations, where plateaus develop. Thus, as acetaldehyde concentration increases, the characteristic shape of the concentration–time trajectory for acetaldehyde more closely resembles the ethanol concentration–time trajectory, and the reaction is limited by the rate of acetaldehyde removal. In healthy *ALDH2*1/*1* individuals, the plateau shape is a result of the balance between the rate of acetaldehyde formation from ethanol and removal. Fig. 4B and 4C show the concentration–time trajectories for ethanol and acetaldehyde, respectively, with and without the reverse reaction accounted for in the rate law for ethanol. By neglecting the reverse reaction, the peak level and area under the curve (a measure of exposure) of ethanol are decreased, whereas the exposure to acetaldehyde is greatly increased. Fig. 4D shows the concentration–time trajectories for ethanol after oral ingestion of ethanol at 0.3 g/kg with an overnight fast and consumption of a standard meal.

4. Conclusions

Findings of the current work demonstrate, for the first time, simultaneous ethanol and acetaldehyde concentration–time profiles. The utility of the model lies in its ability to predict the correct acetaldehyde concentration profiles in different individuals under different experimental conditions when the initial dose and mass of the individual are known. The model least squares parameters coincide strongly with

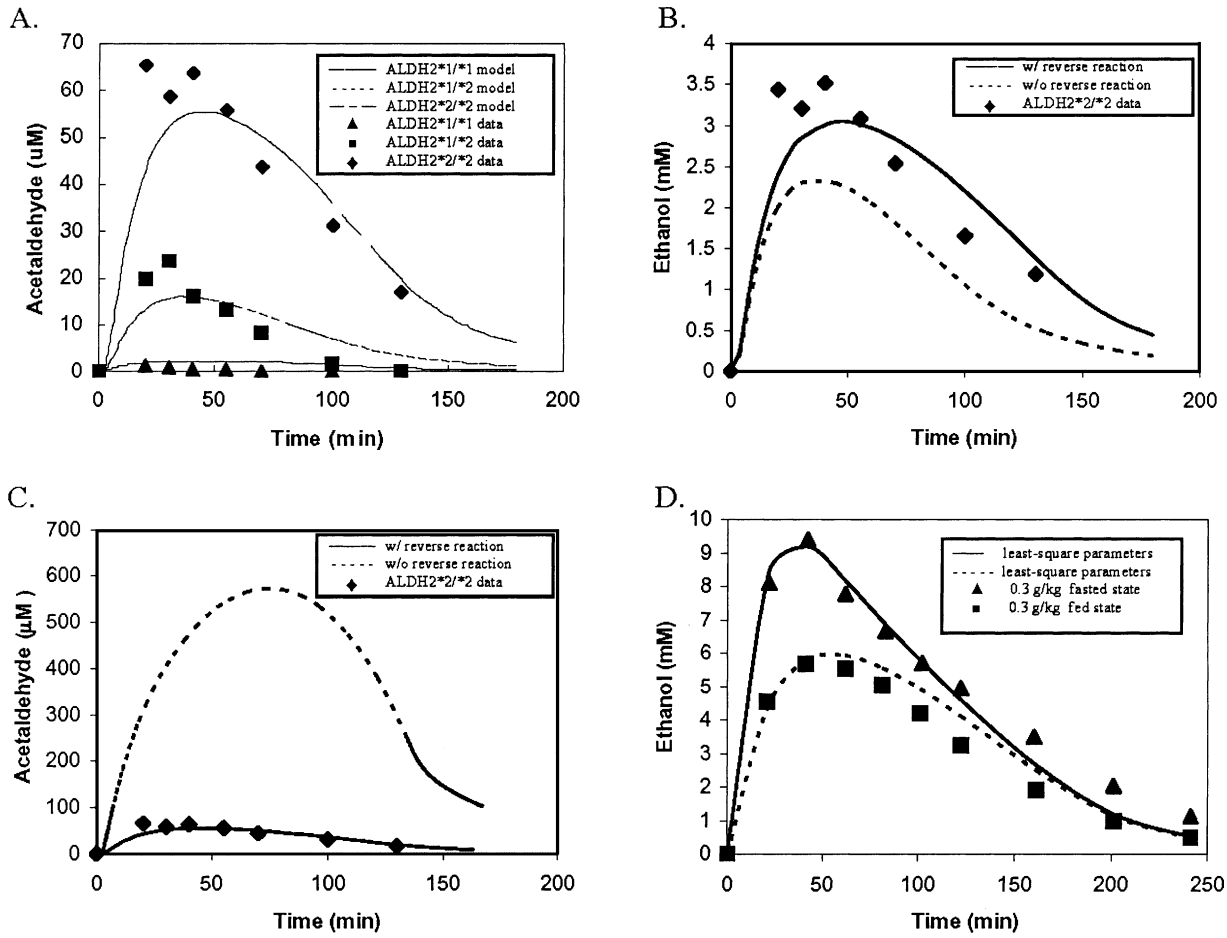

Fig. 4. A. Acetaldehyde concentration data from Peng et al. (1999) after administration of an equivalent 0.2-g/kg dose of ethanol in healthy *ALDH2*1/*1* [data (▲), model (———)]; heterozygous *ALDH2*1/*2* [data (■), model (- - - - -)]; and homozygous *ALDH2*2/*2* [data (◆), model (— – —)] individuals. B. Ethanol concentration data from Peng et al. (1999) after administration of an equivalent 0.2-g/kg dose of ethanol in homozygous *ALDH2*2/*2* [data (◆) shown] individuals. Model curves are shown for homozygous *ALDH2*2/*2* individuals with reverse reaction (——) and without reverse reaction (- - - - -). C. Acetaldehyde concentration data from Peng et al. (1999) after administration of an equivalent 0.2-g/kg dose of ethanol in subjects homozygous *ALDH2*2/*2* (◆). Model curves are shown for subjects homozygous *ALDH2*2/*2* with reverse reaction (——) and without reverse reaction (- - - - -). Note the completely different behavior and peak value of acetaldehyde for the case without the reverse reaction. D. Ethanol concentration data from Lucey et al. (1999) after an overnight fast (▲) and after consumption of a standard meal (■). Also shown are model-predicted blood ethanol curves after an overnight fast (——) and after consumption of a standard meal (- - - - -). Doses were adjusted from the 77.2-kg subjects to the "standard" 69.4-kg man used in the model. Data from Peng et al. (1999), panels A–C: adapted from G. S. Peng, M. F. Wang, C. Y. Chen, S. U. Luu, H. C. Chou, T. K. Li, and S. J. Yin, Involvement of acetaldehyde for full protection against alcoholism by homozygosity of the variant allele of mitochondrial aldehyde dehydrogenase gene in Asians, *Pharmacogenetics 9(4)*, pp. 463–476, fig. 1, copyright 1999, with permission of Lippincott Williams & Wilkins, http://lww.com. Data from Lucey et al. (1999), panel D: adapted with permission from *Journal of Studies on Alcohol*, Vol. 60, pp. 103 110, 1999. Copyright by Alcohol Research Documentation, Inc., Rutgers Center of Alcohol Studies, Piscataway, NJ 08854.

those determined by in vitro experimentation. The high rate of reaction from acetaldehyde to ethanol by means of alcohol dehydrogenase plays a significant role in the kinetics of acetaldehyde and only a minor role in the kinetics of ethanol.

5. Appendix

5.1. Stomach compartment

Ethanol is absorbed primarily by the tissues of the first part of the small intestine (duodenum) and to a lesser extent the tissue lining the stomach (gastric mucosa). The rate of ethanol absorption by the duodenum is between 7.5 and 85 times greater than the rate ethanol enters the blood from the stomach (Wilkinson et al., 1977). Therefore, ethanol entering the duodenum is virtually instantaneously absorbed into the gastrointestinal tissues, and ethanol absorption by the duodenum can be approximated by the rate ethanol is emptied from the stomach into the duodenum. The first-order relation for the change in volume of fluid in the stomach, V_S, with respect to time is given by

$$\left(\frac{dV_S}{dt}\right) = -k_S\,(V_S) \tag{A1}$$

The stomach-emptying rate constant, k_S (min^{-1}), is dependent on the initial dose D (mmol) of ethanol in the system.

5.2. Gastrointestinal compartment

The stomach contents are emptied into the gastrointestinal system, which has a tissue water volume of 2.41 (Derr, 1993). The blood flow rate through the gastrointestinal system is equal to the blood flow rate entering the liver by means of the hepatic portal vein. This flow rate is approximately two thirds of the total blood flow rate to the liver, which is 1,350 ml/min (Levitt & Levitt, 1994). A mass balance on the gastrointestinal compartment gives equations (A2) and (A3) for ethanol and acetaldehyde, respectively:

$$V_G \frac{dC_{GAl}}{dt} = \left(\frac{2}{3} v_L\right)(C_{CAl} - C_{GAl}) + k_S(V_S)(C_{SAl}) \tag{A2}$$

$$V_G \frac{dC_{GAc}}{dt} = \left(\frac{2}{3} v_L\right)(C_{CAc} - C_{GAc}) \tag{A3}$$

In equations (A2) and (A3), V_G is the gastrointestinal system tissue water volume, v_L is the liver flow rate, C_{GAl} and C_{CAl} are the gastrointestinal and central compartment ethanol concentrations, respectively, and C_{GAc} and C_{CAc} are the gastrointestinal and central compartment acetaldehyde concentrations, respectively. V_S is volume of ethanol in stomach compartment, k_S is stomach-emptying rate constant, and C_{SAl} is stomach compartment ethanol concentrations.

5.3. Liver compartment

Ethanol in the blood flows through the hepatic portal vein to the liver after exiting the gastrointestinal compartment. In addition, the liver receives blood from the hepatic artery, which supplies the other one third of the total hepatic blood flow rate. After entering the liver, ethanol is converted into acetaldehyde by the enzyme alcohol dehydrogenase, and acetaldehyde is converted into acetate by acetaldehyde dehydrogenase. Because of the complexity of the forward and reverse reactions in this system, an unsteady-state, physiologically based perfusion liver model is used. Although an analytic solution for the case of irreversible Michaelis–Menten kinetics in a perfused liver is available (Bass et al., 1976), the log mean concentration assumption suggested in that work cannot be used for more complex rate laws with product concentration dependence such as the case presented in this article. When the tubular model (i.e., series of well-mixed compartments) and well-mixed model (i.e., one well-mixed compartment) were compared the concentration–time profiles for ethanol and acetaldehyde corresponded better to the experimental data when the tubular model was used. Furthermore, results of earlier studies supported the suggestion that the rate of clearance and K_m values exhibited a dependence on flow rate when data were fit to a well-mixed compartment, whereas the constants did not exhibit a dependence on flow rate when the perfusion-limited liver model was used (Keiding & Priisholm, 1984). For these reasons, we decided to use the perfusion-limited liver model, and the general mass balance equation for the tubular flow compartment with reaction is

$$\frac{\partial C}{\partial t} + v_L \frac{\partial C}{\partial V_L} = R(C) \text{ with boundary condition}$$

$$C(0,t) = \frac{1}{3} C_C(t) + \frac{2}{3} C_S(t)\,. \tag{A4}$$

C is the concentration of ethanol or acetaldehyde within the liver, whereas C_C and C_S are the concentrations within the central and stomach compartments, respectively. If a backward difference approximation to the spatial derivative is used, this partial differential equation is converted into a set of N ordinary differential equations. This is equivalent to a series of well-mixed reactors, where the output of one reactor becomes the input to the next reactor.

If liver volume is split up into N differential volumes (ΔV_L), equation (A4) becomes equations (A5) through (A7) for ethanol and (A8) through (A10) for acetaldehyde:

$$\text{Compartment } L1\text{: } \Delta V_L \frac{dC_{1Al}}{dt} = v_L\left(\frac{1}{3}C_{CAl} + \frac{2}{3}C_{GAl} - C_{1Al}\right) + r_{Al}(C_{1Al}, C_{1Ac})\Delta V_L \tag{A5}$$

$$\text{Compartment } L2\text{: } \Delta V_L \frac{dC_{2Al}}{dt} = v_L(C_{1Al} - C_{2Al}) + r_{Al}(C_{2Al}, C_{2Ac})\Delta V_L \tag{A6}$$

$$\vdots$$

$$\text{Compartment } LN\text{: } \Delta V_L \frac{dC_{NAl}}{dt} = v_L(C_{(N-1)Al} - C_{NAl}) + r_{Al}(C_{NAl}, C_{NAc})\Delta V_L \tag{A7}$$

$$\text{Compartment } L1\text{: } \Delta V_L \frac{dC_{1Ac}}{dt} = v_L\left(\frac{1}{3}C_{CAc} + \frac{2}{3}C_{GAc} - C_{1Ac}\right) - r_{Al}(C_{1Al}, C_{1Ac})\Delta V_L + r_{Ac}(C_{1Ac})\Delta V_L \tag{A8}$$

$$\text{Compartment } L2\text{: } \Delta V_L \frac{dC_{2Ac}}{dt} = v_L(C_{1Ac} - C_{2Ac}) - r_{Al}(C_{2Al}, C_{2Ac})\Delta V_L + r_{Ac}(C_{2Ac})\Delta V_L \tag{A9}$$

$$\vdots$$

$$\text{Compartment } LN\text{: } \Delta V_L \frac{dC_{NAc}}{dt} = v_L(C_{(N-1)Ac} - C_{NAc}) - r_{Al}(C_{NAl}, C_{NAc})\Delta V_L + r_{Ac}(C_{NAc})\Delta V_L \tag{A10}$$

Ethanol and acetaldehyde exit the liver by means of the hepatic vein into the central compartment with concentrations C_{NAl} and C_{NAc}, respectively.

5.4. Central compartment

The central compartment tissue water volume is the sum of the tissue water volumes of its components: blood, bone, brain, kidneys, lungs, skin, heart, and spleen. The central

compartment is modeled as a well-mixed venous pool with no chemical reaction. The mass balance equations for ethanol and acetaldehyde, respectively, for the central compartment are given by equations (A11) and (A12):

$$V_C\left(\frac{dC_{CAl}}{dt}\right) = -v_L(C_{CAl} - C_{LAl}) - v_M(C_{CAl} - C_{MAl}) \quad \text{(A11)}$$

$$V_C\left(\frac{dC_{CAc}}{dt}\right) = -v_L(C_{CAc} - C_{LAc}) - v_M(C_{CAc} - C_{MAc}) \quad \text{(A12)}$$

V_C is the total water volume for the central compartment, v_L is the liver blood flow rate, and v_M is the blood flow rate to the muscle compartment. C_{MAl} and C_{CAl} are muscle and central compartment ethanol concentrations, respectively. C_{MAc} and C_{CAc} are muscle and central compartment acetaldehyde concentrations, respectively. C_{LAl} and C_{LAc} are liver compartment ethanol and acetaldehyde concentrations, respectively.

5.5. Muscle and fat compartment

The muscle and fat compartment tissue water volume is equal to the sum of tissue water volumes of the muscle and fat tissues. The average perfusion rate for muscle and fat is 0.037 ml/min/ml H_2O, which is significantly smaller than for the other tissues and therefore important to the kinetics of ethanol distribution and elimination. A mass balance on the muscle and fat compartment for ethanol and acetaldehyde gives equations (A13) and (A14), respectively:

$$V_M\left(\frac{dC_{MAl}}{dt}\right) = v_M(C_{CAl} - C_{MAl}) \quad \text{(A13)}$$

$$V_M\left(\frac{dC_{MAc}}{dt}\right) = v_M(C_{CAc} - C_{MAc}) \quad \text{(A14)}$$

V_M is the volume of the muscle and fat compartment, and v_M is the blood flow rate to the muscle and fat compartment. C_{MAl} and C_{CAl} are muscle and central compartment ethanol concentrations, respectively. C_{MAc} and C_{CAc} are muscle and central compartment acetaldehyde concentrations, respectively.

Acknowledgments

We gratefully acknowledge Dr. Richard A. Deitrich (Department of Pharmacology, University of Colorado Health Sciences Center) for helpful discussions.

References

Bass, L., Keiding, S., Winkler, K., & Tygstrup, N. (1976). Enzymatic elimination of substrates flowing through the intact liver. *J Theor Biol 61*, 393–409.

Brien, J. F., & Loomis, C. W. (1983). Pharmacology of acetaldehyde. *Can J Physiol Pharmacol 61*, 1–22.

Condouris, G. A., & Havelin, D. M. (1987). Acetaldehyde and cardiac arrhythmias. *Arch Int Pharmacodyn Ther 285*, 50–59.

Deetz, J. S., Luehr, C. A., & Vallee, B. L. (1984). Human liver alcohol dehydrogenase isozymes: reduction of aldehydes and ketones. *Biochemistry 23*, 6822–6828.

Derr, R. F. (1993). Simulation studies on ethanol metabolism in different human populations with a physiological pharmacokinetic model. *J Pharm Sci 82*, 677–682.

Enomoto, N., Takase, S., Yasuhara, M., & Takada, A. (1991). Acetaldehyde metabolism in different aldehyde dehydrogenase-2 genotypes. *Alcohol Clin Exp Res 15*, 141–144.

Fogler, H. S. (1999). *Elements of Chemical Reaction Engineering* (3rd ed.). Upper Saddle River, NJ: Prentice Hall.

Jones, A. W. (1995). Measuring and reporting the concentration of acetaldehyde in human breath. *Alcohol Alcohol 30*, 271–285.

Jones, A. W., Neiman, J., & Hillbom, M. (1988). Concentration–time profiles of ethanol and acetaldehyde in human volunteers treated with the alcohol-sensitizing drug, calcium carbimide. *Br J Clin Pharmacol 25*, 213–221.

Keiding, S., & Priisholm, K. (1984). Current models of hepatic pharmacokinetics: flow effects on kinetic constants of ethanol elimination in perfused rat liver. *Biochem Pharmacol 33*, 3209–3212.

Levitt, D. G. (2002). PKQuest: measurement of intestinal absorption and first pass metabolism—application to human ethanol pharmacokinetics. *BMC Clin Pharmacol 2*, 4.

Levitt, M. D., & Levitt, D. G. (1994). The critical role of the rate of ethanol absorption in the interpretation of studies purporting to demonstrate gastric metabolism of ethanol. *J Pharmacol Exp Ther 269*, 297–304.

Levitt, M. D., Li, R., DeMaster, E. G., Elson, M., Furne, J., & Levitt, D. G. (1997). Use of measurements of ethanol absorption from stomach and intestine to assess human ethanol metabolism. *Am J Physiol 273(4 Pt 1)*, G951–G957.

Lucey, M. R., Hill, E. M., Young, J. P., Demo-Dananberg, L., & Beresford, T. P. (1999). The influences of age and gender on blood ethanol concentrations in healthy humans. *J Stud Alcohol 60*, 103–110.

Norberg, A. (2001). *Clinical Pharmacokinetics of Intravenous Ethanol: Relationship Between the Ethanol Space and Total Body Water.* Stockholm, Sweden: Karolinska University Press. Available at: http://diss.kib.ki.se/2001/91-7349-053-9/thesis.pdf.

Peng, G. S., Wang, M. F., Chen, C. Y., Luu, S. U., Chou, H. C., Li, T. K., & Yin, S. J. (1999). Involvement of acetaldehyde for full protection against alcoholism by homozygosity of the variant allele of mitochondrial aldehyde dehydrogenase gene in Asians. *Pharmacogenetics 9*, 463–476.

Riveros-Rosas, H., Julian-Sanchez, A., & Pina, E. (1997). Enzymology of ethanol and acetaldehyde metabolism in mammals. *Arch Med Res 28*, 453–471.

Rowland, M., Tozer, T. N., & Rowland, R. (1995). *Clinical Pharmacokinetics: Concepts and Applications* (3rd ed.). Philadelphia, PA: Lippincott, Williams & Wilkins.

Shampine, L. F., & Reichelt, M. W. (1997). The MATLAB ODE suite. *SIAM J Sci Comput 18*, 1–22.

Wang, X., Sheikh, S., Saigal, D., Robinson, L., & Weiner, H. (1996). Heterotetramers of human liver mitochondrial (class 2) aldehyde dehydrogenase expressed in *Escherichia coli*: a model to study the heterotetramers expected to be found in Oriental people. *J Biol Chem 271*, 31172–31178.

Widmark, E. (1932). *Die theoretischen Grundlagen und die praktische Verwendbarkeit der gerichtlich-medizinischen Alkoholbestimmung.* Berlin: Urban & Schwarzenberg.

Wilkinson, P. K., Sedman, A. J., Sakmar, E., Kay, D. R., & Wagner, J. G. (1977). Pharmacokinetics of ethanol after oral administration in the fasting state. *J Pharmacokinet Biopharm 5*, 207–224.

Yamamoto, H., Tanegashima, A., Hosoe, H., & Fukunaga, T. (2000). Fatal acute alcohol intoxication in an ALDH2 heterozygote: a case report. *Forensic Sci Int 112*, 201–207.